Cape Peninsula
University of Technology

FACULTY OF ENGINEERING

MECHANICAL ENGINEERING DEPARTMENT

High strain-rate compressive strain of welded 300WAsteel joints

by

Cletus Mathew Magoda

A Thesis Submitted Towards the Partial Fulfilment Degree of
Master of Technology (M.Tech.)

Supervisor: Prof. Dr. Graeme John Oliver
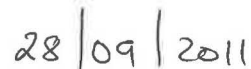M.Sc.(University of Cape Town), Ph.D. (IFTR Warsaw)

Cape Town
February 2011

DECLARATION

I, Cletus Matthew Magoda, declare that the contents of this thesis represent my own unaided work, and that the thesis has not previously been submitted for academic examination towards any qualification. To the best of my knowledge, it contains no copy or paraphrase of work published by another person, except where dully acknowledged in the text. Furthermore, it represents my own opinions and not necessarily those of the Cape Peninsula University of Technology.

28 | 09 | 2011

Signed   **Date**

ACKNOWLEDGEMENTS

ABSTRACT

The split Hopkinson pressure bar (SHPB) test is the most commonly used method for determining material properties at high rates of strain. The theory governing the specifics of Hopkinson bar testing has been around for decades; however, it has only been for the last decade or so that significant data processing advancements have been made. It is the intent of this thesis to offer the insight of application of SHPB to determine the compressive dynamic behaviour for welded low carbon steel (mild steel). It also focuses on the tensile behaviour for unheat-treated and heat-treated welded carbon steel.

The split Hopkinson Pressure bar apparatus consists of two long slender bars that sandwich a short cylindrical specimen between them. By striking the end of a bar, a compressive stress wave is generated that immediately begins to traverse towards the specimen. Upon arrival at the specimen, the wave partially reflects back towards the impact end. The remainder of the wave transmits through the specimen and into the second bar, causing irreversible plastic deformation in the specimen. It is shown that the reflected and transmitted waves are proportional to the specimen's strain rate and stress, respectively. Specimen strain can be determined by integrating the strain rate. By monitoring the strains in the two bars and the specimen's material, stress-strain properties can be calculated.

Several factors influence the accuracy of the results, including the size and type of the data logger, impedance mismatch of the bars with the specimens, the utilization of the appropriate strain gauges and the strain amplifier properties, among others. A particular area of advancement is a new technique to determine the wave's velocity in the specimen with respect to change in medium and mechanical properties, and hence increasing the range of application of SHPB. It is shown that by choosing specimen dimensions based on their impedance, the transmitted stress signal-to-noise ratio can be improved. An in depth discussion of realistic expectations of strain gages is presented, along with closed form solutions validating any claims.

The thesis concludes with an analysis of experimental and predicted results. Several recommendations and conclusions are made with regard to the results obtained and areas of improvement are suggested in order to achieve accurate and more meaningful results.

TABLE OF CONTENTS

CHAPTER ONE: INTRODUCTION

CHAPTER TWO: LITERATURE REVIEW

CHAPTER THREE: THE STRAIN RATE ON THE SPECIMEN

CHAPTER FOUR: COMPRESSIVE WAVES' BEHAVIOUR ON BARS AND SPECIMEN

CHAPTER FIVE: EXPERIMENTAL WORK

vi

LIST OF TABLES

LIST OF FIGURES

APPENDICES

GLOSSARY

Split Hopkinson's Pressure Bar (SHPB)

A device constructed from two long (about 2 meters) round bars as well as a support structure and actuator in which a specimen is mounted and is setup so that the first round bar is used as a hammer and the second round bar is used as an anvil for the test specimen. Strains are measured on the 1st round bar (incident and reflected strains) and on the second round bar (transmitted strains) to determine the material properties of the test specimen.

Strain

The deformation of an object, normalized to its original shape

Strain rate.

Is the Speed at which the deformation occurs when caused by a moving load

Stress

Is the force that material is subjected to per unit of original area.

Heat-affected zone (HAZ)

Is the area of base material, either a metal which has had its microstructure and properties altered by welding or heat intensive cutting operations

Dissimilar metals.

Metals with different physical, thermo and mechanical properties

NOMECLATURE

GREEK LETTERS AND SYMBOLS

ε_i Strain in the incident bar

ε_r Strain in the reflected bar

$\dot{\varepsilon}$ Strain rate [/s]

F_{input} Force on the specimen [N]

F_{output} Reflected impact force from the specimen [N]

C_0, C_L Wave speed on bars [m/s]

ε_t Strain due to transmitted waves

ρ Density of specimen and bars materials [kg/m^3]

u_i Incident wave displacement [m/s]

u_r Reflected wave displacement [m/s]

L_S The Length of the specimen [m]

R_G Resistance of under formed gauge [Ω]

σ_{AVG} Average stress on the specimen [MPa]

Z   Mechanical impedance of the bars [Hz]

P   Applied pressure from the cylinder [MPa]

L_b The length of the base metal [m]

L_{WM} The length of the welded material [m]

L_{HAZ} The length of the Heat Affected Zone [m]

CHAPTER 1

1.1 Motivation

Welded structures may be subjected to high rates of deformation in their operating environment. The microstructure and stress distribution characteristics of welded joints differ from those of the base metal, and the performance of the welded structure is usually limited by the initiation of failure within the Heat Affected Zone (HAZ) of the base metal, particularly within the coarse-grained region of the HAZ adjacent to the weld metal. Therefore, to ensure the reliability of large-scale structures that may be subjected to dynamic impact loading conditions, it is important to evaluate the mechanical properties of their structural materials, including their weld metals, under operating conditions.

The mechanical behaviour of various structural materials under high strain rate impact loading conditions has been studied extensively by means of the Split Hopkinson's Pressure Bar (SHPB) technique or a variety of alternative shock loading apparatus; this has been extensively discussed in the work of Kolsky. H (1949), Daves.E (2006), Hopkinson. B (1914) and Lee.O.S & Kim.M.S (2003). The studies of the mentioned authors have revealed that the strain rate has some degree of influence on the impact properties of most materials. Although the dynamic properties and associated microstructures of different steels have been well documented by Easterling, K.E (1986),Xue.Q.et al (2002) and Chi-FEG,L.et al (2005) in particular, very little has been reported with regard to the impact behaviour and the influence of the strain rate on the welded joint of grade 300WA steel by using the SHPB technique. Grade 300WA steel is a structural steel commonly used in South Africa. Thus, the purpose of this study is to examine the impact behaviour of a grade 300WA steel joint when subjected to the compressive strain rates in the range of 10^2 s^{-1} to 10^5 s^{-1} by using a modified Split Hopkinson Pressure Bar. The effect of the strain rate due to the change of the grain sizes of the weld and the tensile behaviour of the weld are also investigated.

Shuili G, et al (2000) in their research explain that the SHPB technique is one of the most popular experimental techniques for studying the behaviour of materials under high strain rate loading. The principle of this experimental technique is based on the well-known one-dimensional theory of wave propagation in elastic bars and the interaction between a stress pulse and a short cylindrical specimen, which is sandwiched between the input and output bars. The typical SHPB setup as described by Kolsky. H (1949), Hopkinson. B (1914) and

Shuili G, et al (2000), consists of a gas gun, a striker, an input bar and an output bar. A gas gun accelerates the striker bar (projectile). The resulting impact with the input bar produces an elastic, compressive pulse (incident strain). The elastic compressive pulse propagates down the input bar until it reaches the input bar/specimen interface. This compressive pulse then partially reflects back into the input bar (reflected wave) and partially transmits through the specimen into the output bar (transmitted wave). These three stress pulses are associated with respective strains in the bars that are recorded by strain gauges on the input and output bars. The amplitude of the incident pulse depends on the striker velocity.
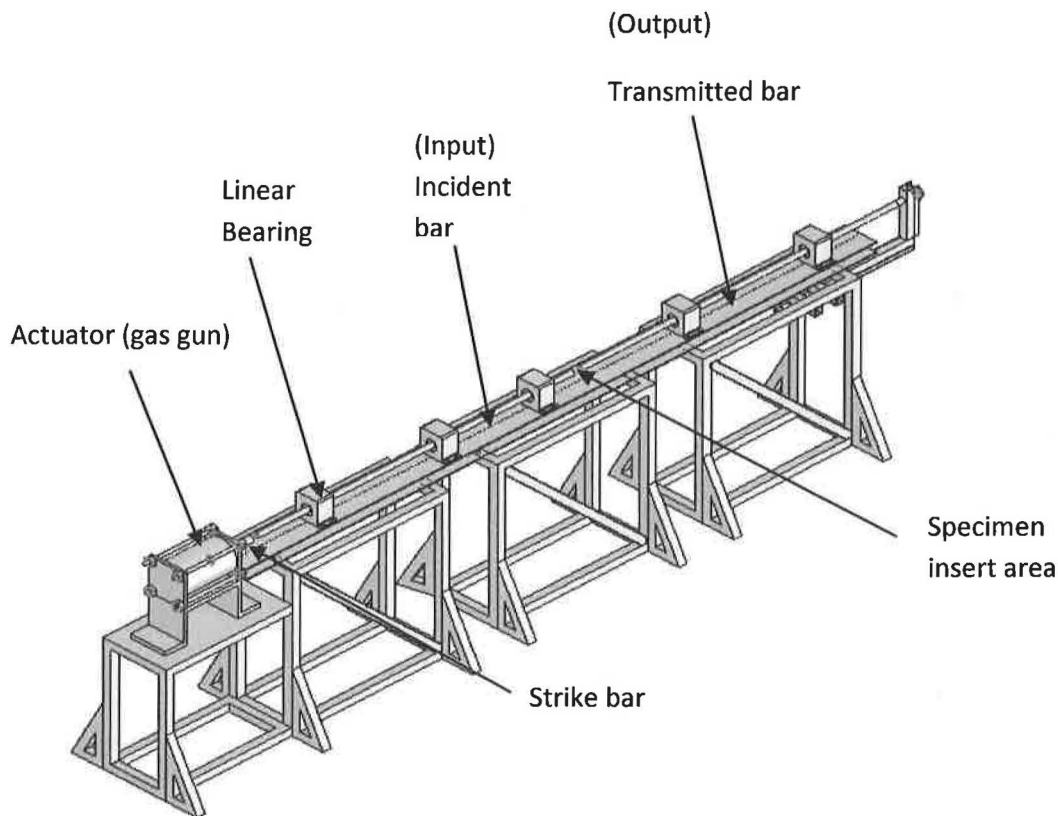
Figure 1.1: Split Hopkinson's Pressure Bar 3D schematic.

1.1.1 Problem Statement

The 300WA Carbon Steel is a commonly used structural steel in the engineering field in South Africa, due to its availability and affordability. It has a variety of uses which includes buildings, bridges, frameworks and vehicles. There are different methods of joining these steel components, one of them being Metal inert gas (MIG) welding. It has been proven within the engineering industry that MIG is a more efficient welding process especially for

different types of steels as compared to other commonly used welding processes. MIG provides a finer HAZ at reduced heat input as compared to traditional oxy-acetylene methods. More importantly MIG is user friendly in so much as the automated machine settings compensate for changes in the process so that less skill and repeatability is required from the operator.

Welding is the most preferable method of joining 300WA Carbon steel. The welded joints are produced to carry loads, extend dimensions and to simplify manufacturing processes by connecting parts into required geometries.

Steel structures are exposed to the external forces that could damage them. As the area around the weld is the weakest part of a welded structure it needs to be analysed in terms of its dynamic response strains produced by external forces.

Residual stresses typically exist on welded joints. Weman Klas (2003) explains that residual stresses always arise in a weld due to the fact that the molten weld metal contracts as it cools. If the parent material cannot withstand this shrinkage due to cooling, then this will result in distortion. It is therefore very important to investigate the residual strain that exists in the weld. Welded joints may be subjected to either quasi-static compression or tension or various dynamic loads.

This research demonstrates the need for the investigation of the weld's strength parameters at High-strain rate conditions. The methodology is demonstrated for a weld of 300WA Carbon Steel exposed to compression loading in a modified Split Hopkinson's Pressure Bar arrangement as well as the tensile behaviour of welded 300WA Carbon Steel.

1.1.2 Sub-Problem

The use of a Split Hopkinson's Pressure Bar was required in order to perform the experiments. To this end, the design, manufacture and commissioning of the pneumatic system and a frame equipped with linear bearings (to allow the incident bar to move freely and the transmission bar to be positioned in alignment with the incident bar) were undertaken.

1.2 Objectives of the research.

1.2.1 Main Objective

To analyze the compressive dynamic and quasi-static tensile behaviour for the welded and un-welded heat-treated and as produced 300WA Carbon steel by using both experimental and analytical methods. A modified SHPB was used for the compressive dynamic test while a tensile testing machine was used to acquire the quasi-static tensile behaviour. With the SHPB, strain gauges (Wheatstone bridge circuits) were used for the recording of strain pulses due to the waves travelling through the incident and transmission bars. The cylindrical specimens underwent a heat treatment process in order to analyse the effect of the change in grain size on the strain rate transmission for both base metal and welded metal.

1.3.2 Specific objectives

- The transmission of the compressive wave can be used to study the weld fusion and it can identify any porous parts of the weld.
- The behaviour of the compressive wave is also indicative of the residual stresses within the weld and the parent materials.
- To identify the deformation of the weld due to a compression force applied at high strain rates.
- To identify the incident and reflected wave velocities.

CHAPTER 2

Literature Review

2.1   INTRODUCTION

This chapter covers the overall development of the Split Hopkinson Pressure Bar apparatus. It also highlights the effect of dynamic loading on the welded and unwelded materials with changes in their grain sizes. A time line approach is taken to summarise the advancements leading to the SHPB apparatus that exist at testing laboratories to date, beginning at the time of its founder/author. Various investigators/researchers have made some significant advances on the SHPB configuration. The second part of this chapter focuses on the effect on the welded and unwelded compressed cylindrical specimens of relatively small diameters compared to the ones of the incident and reflected bars.

2.2   HISTORICAL PESPECTIVE

Hopkinson, B (1914) suggested the split-Hopkinson pressure bar as a way to measure the propagation of a stress pulse in a metal bar. The key components of Hopkinson's apparatus were a means of developing impact like pressure, a long steel rod, a short steel billet, and ballistic pendulum. By impacting one end of the rod, a compressive pressure wave of finite length is generated inside the rod. At the far end of the rod a short steel billet is attached (the specimen under test), held by only a thin layer of grease. Hopkinson's idea was that as the compressive wave traversed down the bar, through the grease joint, and into the billet, the wave would be reflected at the far end as an expansion wave. Since the grease could not withstand any appreciable tensile loads, the billet would fly off with a definite momentum to be measured with a ballistic pendulum. The time over which this momentum acts is the round trip time of the longitudinal wave in the billet. By running several tests of identical magnitude but different lengths of cylindrical billets, a series of pressure-time curves were generated describing the impact event. Hopkinson developed the ability of determining the maximum pressure and total duration of these impact events, and was able to sketch pressure-time curves. With time the application of SHPB became popular as other researchers utilized it for their experiments.

Davies, R.M (1947) in his investigation on the critical study of the Hopkinson pressure bar developed a technique using capacitors. The radial and longitudinal displacement produced by the pressure applied normally to one end of the incident bar is used to produce a change

in the stored electric charge. The output from the capacitor is proportional to the displacement-time relations that are proportional to the pressure-time relations assuming the maximum stress in the bars are under the elastic limit of the material. Using this technique to measure strain tremendously improved the accuracy of Hopkinson's original apparatus which relied on measuring the momentum of a steel billet flying off the end of the pressure bar. The modification of the SHPB did not end there; Kolsky (1949) modified the Hopkinson's original apparatus by adding the second pressure bar, hence the word, split Hopkinson bar, emerged. Instead of attaching the billet at the far end of a bar, Kolsky located the test specimen between two bars. He presented expressions for calculating the specimen's properties, based on the strain histories in the two bars. This technique has become the most widely used testing procedure to date.

2.2.1 Applications of the SHPB in Material testing

Davies and Hunter (1963) investigated the mechanical behaviour of some metals (annealed copper, aluminium, zinc and brass and polymers (polymethylmethacrylate, polyethylene, polyvinyl chloride, polytetra-fluoroethylene, polycapolactam and a filled rubber). The materials were investigated using an SHPB for compressive loading cycles of 30 μsec duration.

Cylindrical specimens, of comparable length and diameter, were sandwiched between two bars and deformed under the action of a compressive stress wave induced into the free end of one of the bars by the detonation of an explosive pellet. Measurements were made of the displacement-time relation for the free end of the other rod, using a parallel plate capacitance microphone.

The mechanical behaviour of the specimen was derived from the analysis of the displacement-time records; in the analysis allowance was made for the non-uniformity of stress and strain inherent in all dynamic testing.

Hartley R.S et al (2007) used the ring compression test to obtain experimental friction factors. He investigated the effect of the surface finish, lubricant, and strain rate on the friction experienced by mild steel, copper and aluminium samples. Numerical simulation was used to assess an energy –based analytical solution, and in particular to establish the effect of neglecting barrelling. The test specimen's microstructure was examined and used to estimate the stress distribution in the specimen during deformation.

Zhao, H (2003) suggested in his findings that when performing SHPB compression tests much emphasis should be on attaining one-dimensional wave propagation. This was

supported by Lee, O.H and Kim, M.S (2003) under the assumption that the induced stresses and strains are constant throughout the bar's cross section. Electrical resistance strain gauges were used for the acquisition of the induced strain on the specimen.

2.2.2 Dynamic and static behavior of Welded steel joints.

According to Xue, Q, et al, (2003), the heat-affected zone (HAZ), which cools at different rates, includes different regions of microstructure and is often considered the source of failure in a welded joint. During welding, base steel close to the fusion area will transform to austenite, martensite, ferrite and/or bainite, depending on the cooling rate and steel composition. These different microstructure phases correspond to different mechanical properties. A weld joint consists of the fusion weld area, the HAZ and base area. Even though some microstructure phases in the HAZ show brittleness and sensitivity to microcracks, one cannot assume that the initiation of the failure is always in the HAZ. The source and mechanisms of failure for a weld joint without pre existing defects, under uniform dynamic loading, still need to be investigated and the strain rate sensitivity of the fracture mechanism cannot be excluded.

Shuili. G, et.al, (2000) considered one-dimensional theory when he investigated the dynamic mechanical properties of a welded joint by means of the SHPB. He found that one-dimensional stress wave theory could be applied for a wave produced when two bars strike each other along their axis. According to the theory of elastic wave reflection and transmission between the different materials' sections, the sound impedance matching among the input pulse bar, the output pulse bar and the test specimen should be taken into account.

Woei-Shyan, L, et al, (2005) investigated the impact properties and residual microstructure of plasma Arc welded 304 LSS weldments by using the SHPB. Results showed that the microstructural characteristics of the weldments were influenced by both, strain rate and by welding current mode. Comparing the evaluation of the microstructure in the base metal and the fusion zone, it was found that a higher dislocation density existed in the fusion zone. Regarding the effect of the strain rate, it is known that a difference exists between a material's mechanical properties when it is subjected to dynamic rather than static loading. In other words the increase in strain rate influences the plastic deformation and fracture characteristics of the material. They came to the conclusion that the strain rate has a significant effect on the martensite transformation and the volume of martensite increases at a higher strain rate as a result of rapid increase in flow stress.

Chao. Y.J et al (2001) used the SHPB to investigate the effect of stir welding on the dynamic properties of AA2024-T3 and AA7075-T7351 welded aluminium alloys. The experimental results showed that friction stir welding reduces the yield stress of the weld metal to below that of the base metal and both materials exhibit the strain rate effect, *i.e.,* the yield stress is higher under higher strain rates;

2.2.3 Energy analysis on a SHPB

Song, B.et al (2005) analysed the energy consumed in deforming the specimen in a SHPB experiment.

At the contact area where the incident stress wave transmits energy to the specimen, the energy of the wave takes the form of strain energy and kinetic energy (bar motion). In other words when the wave reaches the specimen, the energy to deform the specimen comes equally from the strain and kinetic energies associated with the incident wave. He also focused on detailed analyses of the energy transformation and balance. The results led to calculations of the energy absorption during specimen deformation.

2.2.4 Data acquisition system

Marais,S.T. et al (2004) developed a data acquisition system, which enabled to test different materials at different strain rates up to 10^3 s^{-1}. The system was used at 20 MHz and captured 24000 points per channel, proved sufficient to capture the signal of the strain gauge amplifiers. The calibration tests conducted were repeatable and the dynamic calibration factor differed from the theoretical calibration factor by only 5%. The method of determining the Young's modulus and Poisson`s ratio of the specimen's material were determined. The results for the Young's Modulus and Poisson's ratio found to be 1GPa and 0.01 respectively.

Marais (2004) found that the models for the material did not correlate with the actual test data and suspects that the microstructure and the work hardening could be the cause of discrepancy. He further recommended that experiments be performed in future to detect the cause of discrepancy between the test results and the model of the material. The future work on the model of the material should include the effects of work hardening, microstructure and temperature.

2.2.5 Validation of predicted technique

Lambert and Ross (2000) followed up an experimental procedure with a theoretical analysis in order to produce a well-characterized technique for quantifying dynamic fracture properties of quasi-brittle materials. An analytical and experimental investigation of the fracture of concrete was conducted using SHPB. Fracture specimens in the form of notched-cavity splitting tension cylinders were subjected to stress wave loading that produced strain rates nearing 10/s. Fracture parameters were extracted by the application of the two-parameter fracture model, a nonlinear fracture model for quasi-brittle materials. Finite element analysis was verified by the experimental configuration. Ultra-high-speed digital photography was synchronized with the fracture process to provide validation to the predictive technique. Results show that the effective fracture toughness and specimen strength both increase significantly with loading rate. The numeric technique that was validated by the photographic results and the experimental data can be considered as a new tool in determining rate dependent material properties.

2.2.6 The accuracy of the SHPB

The Split Hopkinson pressure bar has become a frequently used technique to measure the uniaxial compressive stress–strain relation of various engineering materials at high strain rate. Using the strain records on incident and transmitter bars the average stress, strain and strain rate histories within the specimen can be calculated by formulae based on one-dimensional wave propagation theory.

Hopkinson, B, (1914) states in his finding that Kolsky's original SHPB analysis was based on the following basic assumptions. (i) The waves propagating in the bars can be described by the one-dimensional wave propagation theory. (ii) The stress and strain fields in the specimen are uniform in its axial direction unless there is a change of medium. (iii) The specimen inertia effect and the friction effect in the compression test are negligible.

Meng, H and Q. M. Li (2009) investigated the accuracy of the SHPB test that is based on the assumption of stress and strain uniformity within the specimen, by introducing friction and specimen size effects. In their findings, they introduced two coefficients to measure the stress uniformity in the axial and radial directions of the specimen, and they have shown that the accuracy of the SHPB test can be correlated to these two stress uniformity coefficients.

2.2.7 Techniques for Measuring Stress-Strain Relations at High Strain Rates

The qualitative dependence of the mechanical behaviour of some materials on strain rate is well known. But the quantitative relation between stress, strain and strain rate has been established for only few materials and for only a limited range. This relation, the so-called constitutive equation, must be known before plasticity or plastic-wave-propagation theory can be used to predict the stress or strain distribution in parts subjected to impact stresses above the yield strength.

A typical SHPB is comprised of long input and output bars with a short specimen placed between them. The impact of the projectile at the free end of the input bar develops a compressive longitudinal incident wave $w_i(t)$. Once this wave reaches the bar specimen interface, a part of it, $w_r(t)$, is reflected, whereas another part goes through the specimen and develops in the output bar as transmitted wave $\dot{w}_t(t)$. The effect of these three basic waves recorded by the strain gauges attached on the input and output bars enable the measurement of forces, wave propagation speed and strains at the two faces of the specimen. This measurement technique is based on the wave propagation theory and on the superposition principle. According to the wave propagation theory, the stress and the particle velocity associated with a single wave can be calculated from the associated strain measured by the strain gauges. The stress and the particle velocity in any given section are calculated from the two waves propagating in opposite directions in this section. When the waves are known at bar–specimen interfaces, the forces and the velocities at both faces of the specimen are given by the following equations

$$F_{input} = S_B E(\varepsilon_i + \varepsilon_r) \qquad V_{input} = C_0(\varepsilon_i - \varepsilon_r) \qquad 2.1$$
$$F_{output} = S_B E \varepsilon_t \qquad V_{output} = C_0 \varepsilon_t \qquad 2.2$$

S_B, E and C_0 are respectively the bar's cross-sectional area, Young's modulus, and the elastic wave speed and ε_i, ε_t and ε_r are the incident, transmitted and reflected strains respectively.

As the three waves are not measured at bar–specimen interfaces in order to avoid their superposition, they have to be shifted from the position of the strain gauges to the specimen faces, in time and distance. This shifting leads to two main perturbations. Firstly, waves

change in their shape on propagating along the bar. Secondly, it is very difficult to find an exact delay in the time shift to ensure that the initiation of the three waves correspond to the same instant.

CHAPTER 3

The Strain rate on the SHPB

3.1   Introduction

Testing of materials at high strain rates is a very specialized branch of experimental mechanics; Klepaczko, J.R (1990). Since the introductory publication of the Split Hopkinson Pressure Bar, as early as 1914, it has been demonstrated that the elastic longitudinal waves in slender rods can be used to measure the detonation pressure of explosives.

A real breakthrough in materials testing at the high split strain rate pressure (10^3 s^{-1}) was brought to attention when Kolsky. H in (1949) instrumented Hopkinson bars with a small wafer specimen in between them to observe the waves through the specimen. Explosives were used to excite the incident compression wave on the free face of the incident bar. The incident compression wave travels along the bar with the elastic wave speed $C_0 = \sqrt{E/\rho}$, where E is the material's young's modulus and ρ is the bar's material density. During the loading period depending on the time of loading the specimen is deformed plastically. A theory of dynamic loading was developed by Kolsky (1949) on the basis of the work of Davies, R.M (1947) where the input data are the three elastic waves, incident, reflected and transmitted.

Hunter S.C (1963) through his work defines the state of material deformations with respect to the high strain rate. One of the defining features of impacts that occur at high velocities is that it is sufficiently large to cause inelastic (and particularly plastic) deformations, and that most of these deformations occur at high strain-rates. These deformations may also lead to large strains and high temperatures. The high-strain-rate behaviour of many materials is defined as the dependence of the flow stress on the strain, strain rate and temperature (σ_f ($\varepsilon, \dot{\varepsilon}$, T)). It is particularly true at high strains and high temperatures. A number of experimental techniques have been developed to measure the properties of materials at high strain-rates. In this section the focus is on the high strain rate measurement for steel base metal and welded steel; heat treated and un-heat treated. Firstly, when speaking of high strain rate, it referrers to how big the deformation is per unit time. Strain rates above 10^2 s^{-1} are classified as high strain rates, strain rates above 10^4 s^{-1} are called very high strain

rates, and strain rates above 10^6 s^{-1} are called ultra high strain rates. Conventionally, strain rates at or below 10^{-3} s^{-1} are considered to represent quasistatic deformations, and strain rates below 10^{-6} s^{-1} are considered to be in the creep domain. In fact, at very high strain rates the yield strength of the material seems to approach the ultimate strength as a limit, but the ductility remains the same. For the experimental work that is discussed in chapter six, a high strain rate of 10^3s^{-1} was utilized when performing the tests.

According to Lindholm.U.S (1964), the application of Split Hopkinson Pressure Bar has a well defined arrangement, where the specimen is placed in contact between the incident and the transmitted bars. For the calculations average strain rate between the two strain gauges that are attached on the two bars should be identified. The average strain rate provides the preferred value for the strain rate of the specimen, defined as the average strain divided by the time over which the straining occurs. Strain indicates displacement per unit length gauge.

3.2   Strain rate on steel weldments.

The heterogeneous microstructure and the presence of residual stress in a welded joint make its behaviour under dynamic loading unpredictable.

The high strain rate of the weld has received many definitions from Woei-Shyan, L, et al, (2005). Xue Q.et al, (2003) and Shuili G, et al (2000). These definitions include, the rate at which the weld joint is compressed relative to its initial dimensions is termed as "the strain rate of the weld"; the strain rate of the weld is "the dynamic impact strength" and "the rate of strain energy absorbed by the weld". The influence of high strain rate on the compression properties of the weld merely depends on the thermo-mechanical properties of the host material and the impacting force used. Welded joints are regarded as the points in a structure that failure is likely to occur due to a combination of factors, including residual stress induced when welding takes place. Hence the study on the welded joints under dynamic loading is of importance.

3.3   Mathematical description of stress and strain rate for the specimen.

In a Split Hopkinson Pressure bar apparatus, when the striker hits the incident bar, a compression wave with a specific amplitude and length moves through its length. The compressive wave is a function of the velocity and shape of the striker. When the wave reaches the end of the incident bar, a fraction of it is transmitted to the specimen and some is reflected. This is due to the possible mismatch in the cross-sectional area and acoustic impedance between the incident bar and the specimen. The wave transmitted by the

specimen to the transmitted bar is a function of specimen material properties. The above explanation of wave propagation and the factors affecting it can be represented mathematically by using the one-dimensional theory for wave propagation.

According to the findings by Zhou,X.Q and Hao,H (2008), the use of one-dimensional wave propagation helps to determine high rate stress-strain curves from measurements of strain gauges in the incident and transmitted bars. Equation 3.2 is a solution to the second order differential equation given by the one-dimensional wave equation.

$$\frac{\partial^2 u}{\partial x^2} = \frac{1}{c^2} \frac{\partial^2 u}{\partial t^2}$$
(3.1)

$$u_T = u_i + u_r$$
(3.2)

Where, c is the acoustic speed in the material in the incident and transmitted bars. u_T, u_i and u_r are the total, the incident and the reflected wave displacements that occur in the incident bar. Assuming a one-dimensional system with respect to time, the strain rate in the incident bar can be determined by differentiating the wave displacement equation 3.2 and the following equation can be written.

$$\dot{u}_t = c(-\varepsilon_i + \varepsilon_r)$$
(3.3)

$\dot{u}_t$, ε_i and ε_r are the displacement rate, incident and reflected strains respectively. In the split Hopkinson Pressure Bar test before the reflection occurs at the end of the transmitted bar, only a single wave travels along it. With this assumption, equations 3.3 can be written as:

$$\dot{u}_t = -c\varepsilon_t$$
(3.4)

ε_t is the transmitted strain and $\dot{u}_t$ is the wave displacement rate in the transmitted bar. Figure 3.1 gives a view of the incident bar, the specimen and the transmitted bar.

14
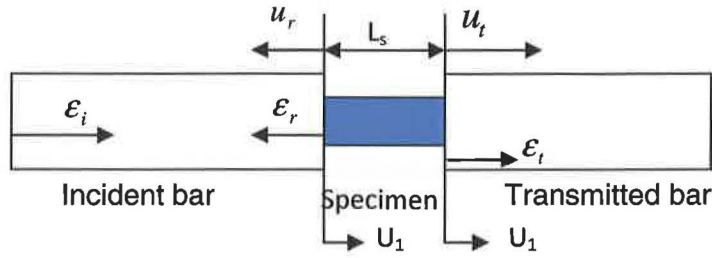
Figure 3.1: Expanded view of the incident bar, specimen and transmitted bar

Equation 3.5 gives the strain rate in the specimen. Using equations 3.1, 3.2 and 3.3, equation 3.6 can be obtained.

$$\dot{\varepsilon}_{specimen} = \frac{\left(\dot{u}_1 - \dot{u}_2\right)}{l_s} \tag{3.5}$$

$$\dot{\varepsilon}_{specimen} = \frac{c}{l_s}\left(\varepsilon_i - \varepsilon_r + \varepsilon_t\right) \tag{3.6}$$

l_s is the instantaneous length of the specimen and $\dot{\varepsilon}_{specimen}$ is the strain rate in the specimen. Using the definition of the forces in the incident $\left[F_i = AE(\varepsilon_i + \varepsilon_r)\right]$ and transmitted bars $\left[F_t = AE\varepsilon_t\right]$ and assuming that the specimen deforms uniformly, the transmitted strain can now be expressed as:

$$\varepsilon_t = \varepsilon_i + \varepsilon_r \tag{3.7}$$

The relationship expressing the strain rate in the specimen, given by equation 3.8 below, can be obtained by substituting equation 3.7 into equation 3.6. Also, the stress in the specimen can be calculated by dividing the force in the transmitted bar by the cross-sectional area of the specimen and equation 3.9 can be obtained.

$$\dot{\varepsilon}_{specimen} = \frac{2c\varepsilon_i}{l_s} \tag{3.8}$$

$$\sigma_{specimen}(t) = \frac{AE\varepsilon_t}{A_s} \tag{3.9}$$

where A is the cross-sectional area of the incident and transmitted bars, E is the Young's modulus of the bars and A_s is the cross-sectional area of the specimen.

3.4   Specimen's Stress

The average stress in the cylindrical specimen can be expressed in terms of the forces exerted on Incident bar-Specimen and Transmitted-Specimen Interfaces, this is according to Woldesenbet, E. and Vinson, J.(1997).
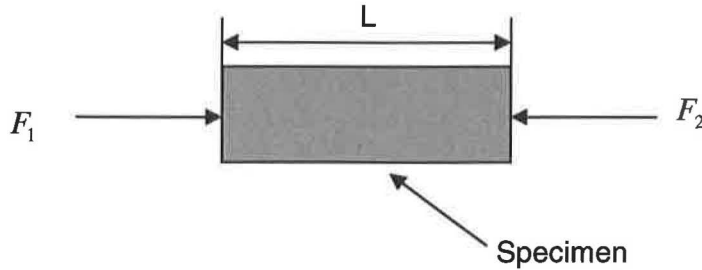
Figure 3.2: Schematic of the cylindrical specimen

When the specimen is sandwiched between the incident and transmitted bars, forces F_1 and F_2 exist on this specimen of instantaneous diameter D_s. The average force on the specimen is given by

$$F_{AVG}(t) = \frac{F_1 + F_2}{2}$$

(3.10)

and therefore the average stress on the cylindrical specimen is given by

$$\sigma_{AVG}(t) = \frac{F_{AVG}}{\frac{\pi D_s^2}{4}}$$

(3.11)

The two forces F_1 and F_2 acting on the specimen surfaces are due to the incident and transmitted bars. For dynamic equilibrium in the specimen, the strains of the incident and transmitted pressure bars are used to express the forces on the specimen.

$$F_1 = E[\varepsilon_i + \varepsilon_r]\frac{\pi D_{BAR}^2}{4}$$

(3.12)

16

$$F_2 = E\varepsilon_t \frac{\pi D_{BAR}{}^2}{4} \qquad\qquad (3.13)$$

D_{BAR} is the diameter of the pressure bars. Substituting equations 3.10, 3.12, and 3.13 into equation 3.11 results in an expression for the average stress on the specimen in terms of the pressure bar strains.

$$\sigma_{AVG} = \frac{E D_{BAR}{}^2}{2 D_S{}^2}\left[\varepsilon_i + \varepsilon_r + \varepsilon_t\right] \qquad\qquad (3.14)$$

If the specimen deforms uniformly, the strain in the incident bar is equal to the strain in the transmitter bar

$$\varepsilon_i + \varepsilon_r = \varepsilon_t \qquad\qquad (3.15)$$

and the expression for the average specimen stress can be reduced to

$$\sigma_{AVG} = \frac{E D_{BAR}{}^2}{D_S{}^2}\left[\varepsilon_i + \varepsilon_r\right] \qquad\qquad (3.16)$$

This equation shows that the specimen stress is proportional to the amplitude of the strain transmitted through the specimen into the transmitter bar.

3.5   Compression wave analysis on the SHPB

Kolsky, H (1945) proposed a new configuration of two Hopkinson bars in order to determine the $\sigma(\varepsilon)$ relation of materials when the time of deformation is short, typically from $20\,\mu s$ to $500\,\mu s$, this means a high strain rate. In Kolsky's apparatus a short cylindrical specimen is placed in between two hard bars (discussed in chapter one).

Kepaczko, J (1999) characterized the behaviour of the waves transmitted on the Kolsky bars as elastic and that they depend on the bars' and specimen's diameters. The difference of effective impedances and yield stresses between a hard bar and a soft specimen is high if the specimen diameter is slightly smaller than the bar diameter, when an impact strikes an incident bar, part of the incident wave is reflected as a tension wave and the other part is

transmitted through the specimen into the transmitter bar. During the wave transmission the specimen is deformed plastically.

The effective strain rate in an element is dependent not only on the rate of loading but also on such factors as the shape and dimensions of the specimen. If it is assumed that the specimen stretches uniformly (no necking/localization) and in a uniaxial test that the strain rate is spatially uniform over the whole specimen, then the following is true:

- engineering   strain rate $= \dfrac{\varepsilon}{t} = \dfrac{r}{L} = \dot{\varepsilon}$

- change in length $= \Delta L = r \times time = \varepsilon * L$

- engineering strain $= \dfrac{\Delta L}{L} = \dfrac{r \times time}{L} = \varepsilon$

- true strain $= \ln(1+ \text{engineering strain}) = \ln\left(1+ \dfrac{r \times time}{L}\right)$

- true (effective) strain rate varies with time $= \dfrac{d\varepsilon}{dt} = [\ln\left(1+ \dfrac{r \times time2}{L}\right) - \ln\left(1+ \dfrac{r \times time2}{L}\right)]$ / (time 2-time 1)

    L = length of specimen in loaded direction; r = rate of loading

Sobczyk, K and Trebicki, J (2004) strongly linked the presence of Residual stresses in a weld, which arise due to difference in cooling rate between the fusion zone and the parental material. Residual stresses in a fusion zone are normally tensile and proven to be in magnitude very close to the yield stress. Residual stresses cause brittleness around the heat affected zone.

CHAPTER 4

Compressive waves' behaviour on SHPB bars and specimen

4.1. Introduction

Lee O.S and Kim, M.S. (2003) defined SHPB in terms of its functionality. In a split Hopkinson bar, when the striker hits the incident bar, a rectangular compression wave with a specific amplitude and length moves through the length of the incident bar. The compressive wave is a function of the velocity and shape of the striker. When the wave reaches the end of the incident bar, a fraction of it is transmitted to the specimen and some is reflected. This is due to the mismatch in the cross-sectional area and acoustic impedance between the bars and the specimen. The wave transmitted by the specimen to the transmitted bar is a function of specimen material properties.

Change in grain sizes of the material affect the continuity and the speed on which the waves propagate through bars as well as specimen. Heat treatment (annealing) is used to obtain this change in grain sizes on both base metal and weld. The rate of cooling for the heat treated specimen is so significant towards obtaining different sizes. The heat treated specimens were cooled within the furnace. Chapter 6 explains more on microstructure description for the heated specimens.

This chapter explains the effect of grain sizes on wave's propagation on different medium. The main focus is on base metal (low carbon steel), the heat affected zone and the weld.

The nature of the waves propagated, velocity and the balance forces for the incident, reflected and transmitted waves are discussed.

4.2. Longitudinal Waves Propagation in Bars

Newton's Second Principle defines the inertia due to this phenomenon as a sharply applied pressure or velocity into one part of a solid material is transmitted to other parts. This is of course the wave propagation, the phenomenon which occurs in gases, liquids and solids.

Julian L. Davis (2000) explains in his research that the phenomenon of wave propagation in bars is governed by the one-dimensional wave propagation that has been defined and derived mathematically to obtain a wave equation in terms of velocity and specimen displacement. The theory was also supported by Meng H and Li.Q.M (2003) by indicating that the application of this theory in elastic bars, wave propagation is not distorted by wave dispersion and attenuation.

It has been indicated by Deshpande, V .S, Fleck, N.A. (2000), Hopkinson B. (1914), Lindholm, U.S. (1964), that the propagation of longitudinal waves in one-dimensional bar theory can be represented mathematically by letting its longitudinal axis be the x axis. The displacement is vector $u = u(u(x,t),0,0\ ))$, since there is plane wave propagation. Considering the equation of motion, where $u = w = 0$; the one-dimensional wave equation for displacement is

$$c_L^{\ 2}\, u_{xx} = u_{tt} \qquad\qquad\qquad\qquad [4.1]$$

$c_L = \sqrt{\dfrac{E}{\rho}}$ (Wave propagation speed), u_{xx} is the displacement in x axis and u_{tt} is the particle acceleration. The first principle approach should be used to derive the one-dimensional wave equation for the bar, since it yields the correct expression for wave velocity.

On the modified Split Hopkinson Bar, two precision resistant strain gauges (120Ω) have been attached on both bars (incident and transmitted). When the input bar is impacted with the striker bar, all three types of pulses ($\varepsilon_i, \varepsilon_r, \varepsilon_t,$) are generated and recorded by strain gauges attached on bars.

The incident bar, Reflected bar and the specimen have discontinuities that have significant effects on wave propagation. The common discontinuities include the variation on cross sectional diameters and The Heat Affected Zone of the welded specimen on which the fusion is expected to be not as accurate as unwelded metal.

For Split Hopkinson Pressure Bar applications, the variation in cross section diameters is mostly a step change, usually occurring at the Incident-Specimen interface.

Moreover there is an Impedance change is expected to take place on the weld due to change in mechanical and physical behaviour of the weld. Below is the incident, reflected and transmitted waves propagation trend for the bars and specimen.
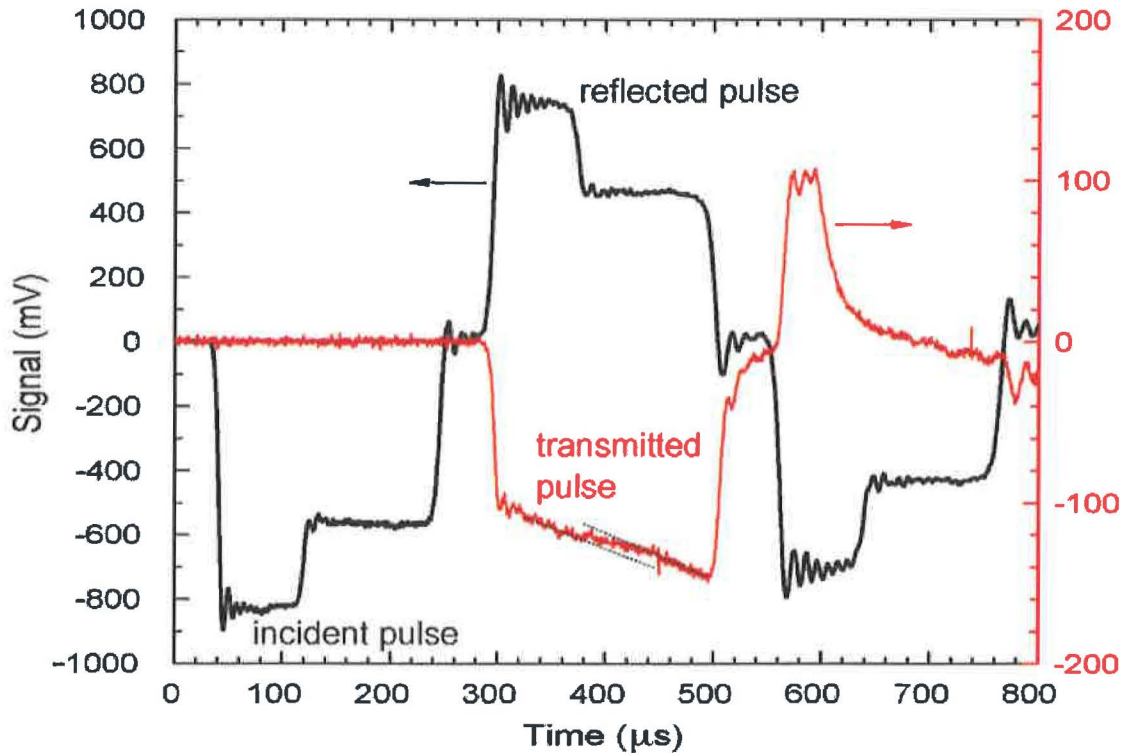
Figure 4.1: Pulse generated in the incident and reflected bars after impact (Kapoor, 2008)

4.3. Longitudinal Waves Propagation in weldments

Waves are regarded as the means of transferring information through medium, in this case, through the bars and the weld. The propagation of waves through two welded cylindrical specimens of diameter 16mm and length of 20mm is the area of interest on this section. The welded specimen provides three media of wave transfer which are the two pieces of base metal and the weld. Waves' propagation through material depends on the mechanical and physical properties of that material, hence the weld is treated as a medium with different properties. This finding was supported by Yaowu Shi, et al (2004) which shows that the macroscopically mechanical heterogeneity of the welds may have an important influence on the fracture toughness of the Heat Affected Zone than the meso-heterogeneity in the reheated course grained HAZ.

Jiang, H. et al (2006) through their research have identified that the steel welds have an equiaxed microstructure with a 1 mm grain size in the fusion zone, 100 /spl mu/m in the heat affected zone (HAZ) and 50 /spl mu/m in the parent metal. The fusion zone had slightly higher microhardness values despite having a large grain size, while the unaffected material had the lowest microhardness.

The mechanical properties of the weld and HAZ are different from the parent material due to differences in microstructure and impurity atom content. For steel weld, it is assumed to be more or less the same with the base metal.

Wave propagation follows the continuity of mechanical properties of the medium, there fore the welded specimen does have a discontinuity of mechanical properties.

4.4.   The effect of grain sizes on mechanical properties of the base metal

The rate at which the metals can be deformed (strain rate) is influenced by so many considerable factors. These factors include impacting force, material properties (hardness, toughness etc) which are the results of grain sizes and distribution in a metal.

Shankaranarayan, H and Varme, K.S (1995) in their research on strain rate and grain sizes effect on substructures concluded that the flow stress values for small grain sizes were higher than that of bigger grain sizes. Crystals (grains) grow as a metal cools. The slower the metal is cooled, the larger the grain size will be. Composition also affects the grain size, since it can affect the tendency of metals to form new grains versus continuing to add to existing grains. In the case of alloys, cooling can also result in the separation of phases - crystallization of more than one type of grain at the same time, or the separation of grains into more than one phase as the material cools. In general, larger grain size makes it easier to work or deform a metal, while finer grain size makes the metal more rigid.

Muszka.K, et al (2009) investigated the Study of the effect of the grain size on the dynamic mechanical properties of microalloyed steels and the results concluded that the effect of grain size on the mechanical behaviour for C-Mn Steel shows that the micro structure changes and, first of all grain refinement caused the improvement in mechanical properties for that particular steel. It has been indicated that the yield ratio increases with decreasing size. It is well understood that the levels of mechanical behaviour discrepancies under dynamic loading conditions depend on chemical composition of steel and applied processing parameters.

4.5. The effect of grain sizes on mechanical properties of the Heat Affected Zone

The heat affected zone for this case is considered as the medium which is situated between the base metal and the weld. Upon cooling, the micro-structure is partially changed. Therefore, different micro structural sub-zones in the heat-affected zone (HAZ) are the spheroidized zone, partially transformed zone, grain-refined zone and grain-coarsened zone. The microstructures formed in both weld metal and HAZ play an important role in controlling the mechanical properties of the welding zone. On the other hand, heat input is directly effective on the microstructures formed in weld metal and HAZ. The typical microstructure formed in weld metal (WM) of low carbon steels consists of grain boundary ferrite (GBF), Widmanstäten ferrite (WF) (side plates), acicular ferrite (AF) and microphases (a small amount of martensite (M), retained austenite (RA) or degenerate pearlite (P)) depending on the cooling rate. In addition, it is reported that bainite (B) was formed in the weld metal. The phases formed in HAZ have the same formation mechanism as the phases occurring in weld metal except for acicular ferrite. The acicular ferrite grains form in weld metal since they nucleate on non-metallic inclusions. The acicular ferrite is of considerable importance because it provides a relatively tough and strong microstructure. It has in the past been accepted that grain boundary ferrite is detrimental to weld metal toughness, since it offers little resistance to cleavage crack propagation. However, it is a reconstructive transformation involving the diffusion of all atoms, so that grains of grain boundary ferrite can grow freely.

4.6. The mechanical Properties of steel welds

According to Aitchson, L and Pumphrey, W (1953), the mechanical properties of a weld are determined by the chemical compositions of the posited weld-metal and the parent metal, by the soundness of the weld, and by any heat-treatment which is given after the completion of the welding operation. Other things being equal, however, the strength of a weld is determined by the strength of the weld-metal.

For the lower-carbon steels, welding can be controlled to produce weld-metal which possesses very similar mechanical properties to those of the base metal.

For instance, the mechanical properties of low carbon-content weld-metal, deposited by arc-welding and using coated electrodes, are similar, over a wide range of temperature to those of plain-carbon steel containing approximately 0.25% of carbon.

4.7. Waves propagation on the steel weld with change in grain sizes

The mechanical and physical properties of the steel weld have close similarities with that of base metal. The welded joints are very heterogeneous in mechanical properties because of their heterogeneity in micro structure, discontinuous in geometrical shape and welding residual stress. This affects the continuous flow of pulses when allowed to flow through. The structural change of the medium has a significant effect towards the magnitude and stability of the waves/pulses.

Wuan-Yuan Hsiao, et al (2008) in their findings indicated that the heterogeneous microstructure generated by welding not only changes the chemical composition but also manufactures a weld with non-uniform mechanical properties. The cooling rate has an important role in determining the extent of transformation. A slow cooling rate produces more austenite formation while a fast cooling rate produces less austenite constituent.

According to research done by Xue,Q et al (2002) on the constitutive response on welded HSLA 100 steel, the weld has a typical microstructure of proeutectoid ferrite, polygonal widmanstatten and circular ferrite, as well as bainite and martensite. The circular ferrite is considered to be a toughening phase which makes a weld have grains that do not easily allow the propagation of stress waves through it.

The heat-affected zone (HAZ) is cooled at different rates and includes different regions of microstructure and is considered to be the source of failure in a welded joint. During the welding thermal cycle, base steel, close to the fusion area, will transform to austenite, martensite, ferrite and/or bainite, depending on the cooling rate and steel composition. These different phase microstructures correspond to different mechanical properties. A weld joint consists of fusion weld area, the HAZ and base area (unwelded). Even though some phases in the HAZ show their brittleness and sensitivity to the micro cracks, one cannot assume that the initiation of the failure is always in the HAZ. The source and mechanisms of failure for a weld joint without pre-defects under uniform dynamic loading still need to be investigated and the strain rate sensitivity of fracture mechanism cannot be excluded.

4.8 Waves propagation through different media.

The intent of this section is to describe the behaviour of a wave as it encounters a discontinuity i.e. incident bar to base metal specimen to the weld the base metal. Below is the schematic of change in media and material properties of the welded specimen.
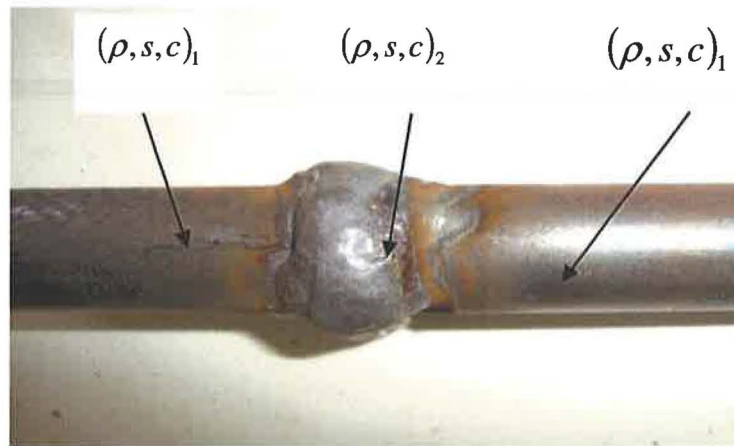
Figure 4.2: Schematic of the change in material properties for the welded specimen

Lee.O.S & Kim.M.S, (2003) in their findings discovered that the most commonly encountered discontinuities in the split Hopkinson bar testing are step changes in cross sectional areas and material properties. In this research, the discontinuity due to weld properties is looked at intensively. Waves encountering discontinuities are usually examined in terms of impedance. Impedance is defined as the ratio of the driving force to the velocity at a point in a structure (pressure bar in this case). Equation 4.1 is an expression for the mechanical impedance of the bars used in Hopkinson bar testing.

$$Z = \frac{F}{V} = s\rho C_0 \qquad\qquad (4.2)$$

The variables ρ, s, and C_0 are the mass density, cross sectional area, and longitudinal wave velocity, respectively. The product ρc has a constant value for a given material; it is often convenient for the two to be grouped together as one term. Notice that all of the impedance variables are physical properties; the impact event does not affect the impedance of the bars. Further notice that for any given bar material an impedance change can only occur by changing the cross sectional area.

Typically, discontinuities occur at the pressure bar – specimen interfaces. Since a wide range of materials may be under investigation, it is important to understand how waves respond to changes in media. Consider the familiar scenario in which one type of solid is sandwiched between two dissimilar solids of different cross sectional areas, depicted in figure 4.3.

$(\rho,s,c)_1$ $(\rho,s,c)_2$ $(\rho,s,c)_3$

A_2

A_1

A_3

B_1 B_2

$X=0$ $x=L$

$+X$
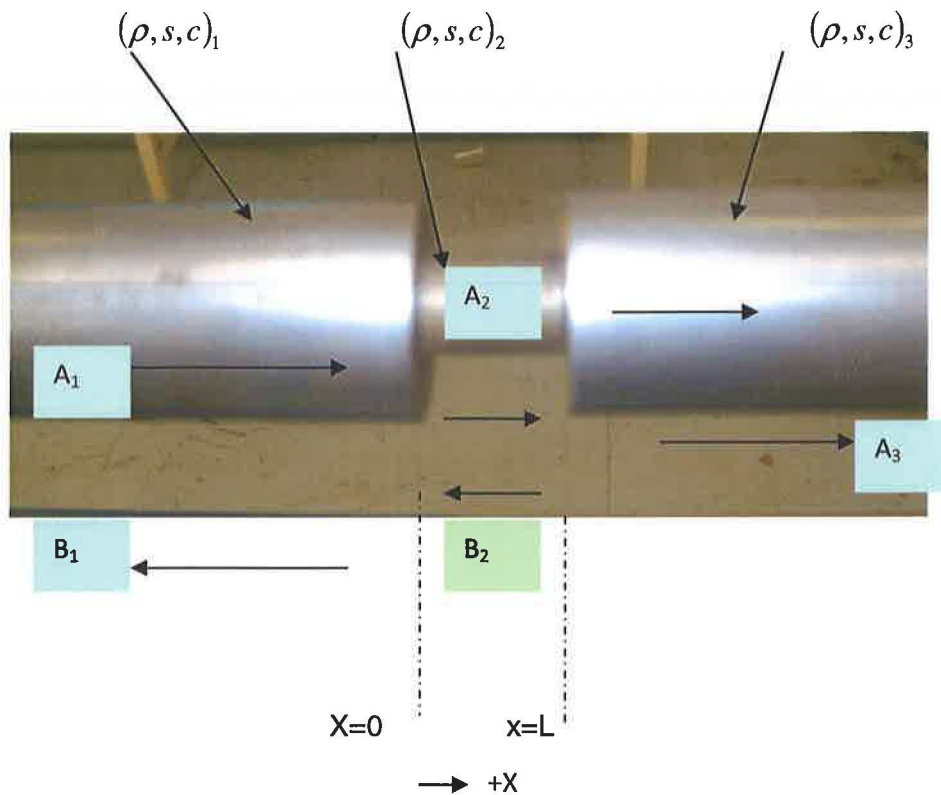
Figure 4.3: Schematic of the wave's propagation through the SHPB and specimen

Variables ρ, s, and c are the same as those used in equation 4.1. The terms A_1-A_3 and B_1-B_2 denote the stress amplitudes for waves travelling to the right and to the left, respectively. At interface 1 ($X=0$), wave A_1 is partially reflected and transmitted as waves B_1 and A_2, respectively. At interface 2 ($X=L$), wave A_2 is partially reflected and transmitted as waves B_2 and A_3, respectively. The level of reflection or transmission is dependent on the impedance mismatch at each interface. The figure (4.4) below illustrates waves travel trend on both the bars and the specimen.
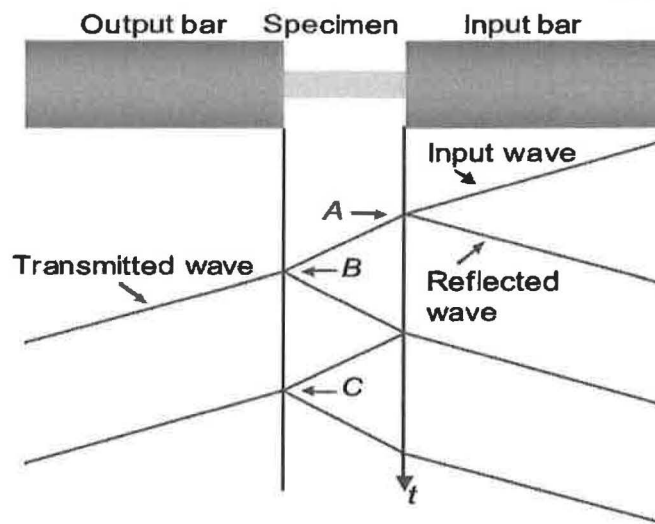
Figure 4.4: Lagrange diagram of the stress waves in a SHPB specimen (Saviour 2009)

To quantify the stress amplitude variables and hence the amount, a wave is reflected and transmitted at the bars and specimen interfaces requires an understanding of the dynamics at each interface. At each of the two pressure bar –specimen interfaces, the velocity of each material just to the left and right of the interface must be equal, since they are in intimate contact at all times. The forces just to the left and right of each interface must balance one another to satisfy the equilibrium. By recognizing that, these conditions must be true, equations describing the interface effects on wave propagation may be written. The system of equations described for the un-welded specimen for interfaces one and two are shown in Equations 4.3, 4.4, 4.5 and 4.6 below.

Interface 1: Incident bar- specimen interface (X=0)
Continuity of velocity

$$\frac{A_1 - B_1}{(\rho c)_1} = \frac{A_2}{(\rho c)_2}$$ (4.3)

Force Balance

$$S_1(A_1 + B_1) = S_2 A_2$$ (4.4)

Interface 2: Transmission bar- specimen interface (X=L)
Continuity of velocity

$$\frac{A_2 - B_2}{(\rho c)_2} = \frac{A_3}{(\rho c)_3}$$ (4.5)

Force Balance

$$S_2(A_2 + B_2) = S_3 A_3$$ (4.6)

When the incident pulse arrives at the specimen a compressive loading wave is generated inside the specimen. The compressive loading wave propagates through the specimen and arrives at the specimen output-bar interface. However, a welded specimen has two median in which waves propagate through. The nature of the impedance within the weld should be smaller than that of the base metal, due to fact that there is a heterogeneous microstructure.

By design, the specimen's impedance is smaller than the impedance of the bars surrounding the specimen on both sides. Since the output bar has higher impedance than the specimen itself, the wave that reflects from the specimen/output-bar interface remains a loading wave, resulting in an even higher compressive stress. This wave now arrives at the welded specimen with higher compressive stress in addition to the already existing stress on the weld (i.e. residual stress and engineering stress). The waves will therefore arrive at specimen/input-bar interface, again sees higher impedance and again reflects as a loading wave, resulting in a further increase in the compressive stress. This process continues until the stress within the specimen reaches a value that is sufficiently high to generate inelastic strains, resulting in finite plastic flow of the specimen under the compressive loading. Once substantial plastic flow of the specimen material has commenced, further wave propagation within the specimen may be neglected, since the amplitude of the subsequent wave fronts will be very small. Thus at these later times the stress within the specimen is essentially uniform; the stress is said to have equilibrated. If the boundary conditions are frictionless, the specimen stress is also uniaxial.
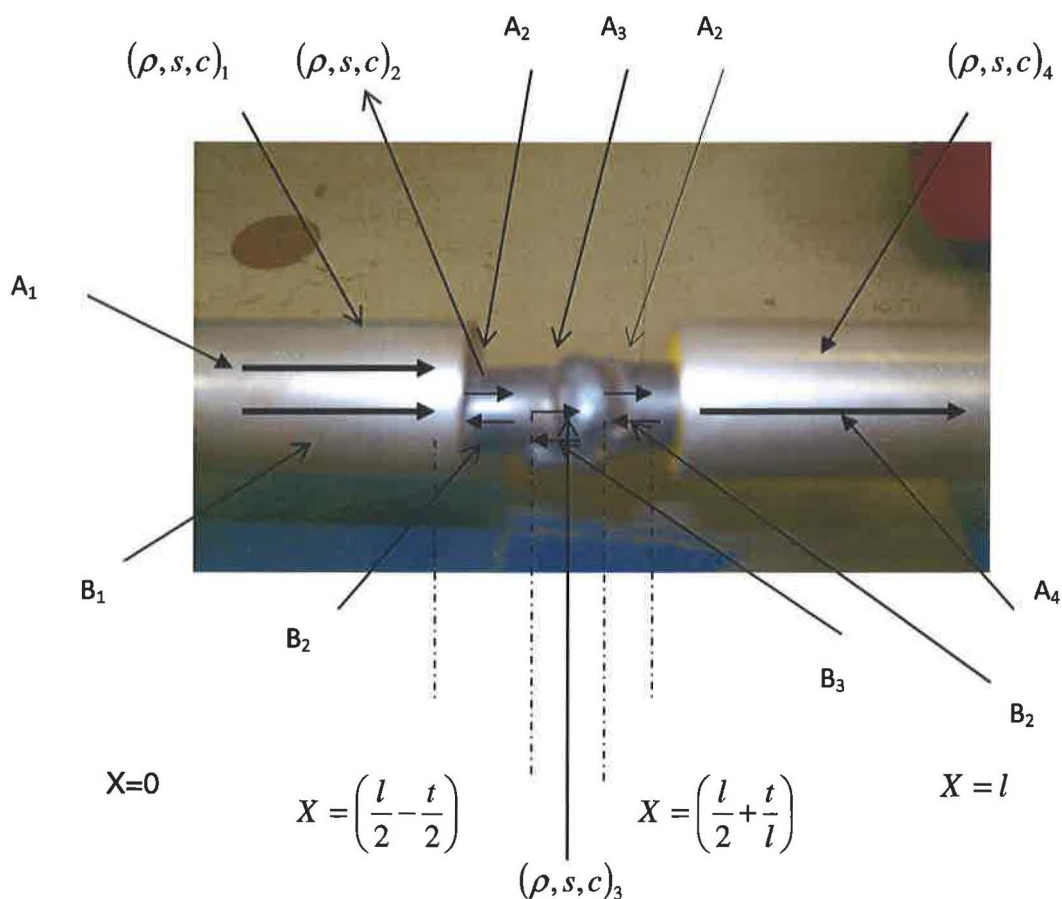
Figure 4.5: Schematic of the wave's propagation through the SPHB and welded specimen

For the welded specimens the weld was treated as a different medium that affected the stress and impulse propagation. As discussed previously, the mechanical properties of the steel weld are not significantly different from the base metal and HAZ. It was expected that the reflection of pulses at the weld is not of the higher magnitude compared to that from interfaces. Incident bar-specimen and specimen-transmitted bar interfaces have higher amounts of reflected impulses due to mismatch in terms of their sizes and properties. The compressive stress increases from the specimen-reflected bar interface towards incident bar- specimen interface through specimen. For this matter, the compressive stress is higher at the incident bar- specimen interface for welded specimen test that for un-welded specimen test. Equations 4.7, 4.8, 4.9, 4.10 represent the compressive stress distribution for the welded specimen test. Refer to figure 4.3 for the detailed allocation of stress zones for the tested welded specimen by SHPB.

Interface 1: Incident bar- specimen interface (X=0)
Continuity of velocity
$$\frac{A_1 - B_1}{(\rho c)_1} = \frac{A_2}{(\rho c)_2} = \frac{A_3}{(\rho c)_3} \qquad (4.7)$$
Force Balance
$$S_1(A_1 + B_1) = S_2(A_2 + B_2) + S_3(A_3 + B_3) \qquad (4.8)$$

Figure 4.6: Mathematical description for the force and velocity within Incident-Specimen interface.

Interface 2: Transmission bar- specimen interface (X=L)
Continuity of velocity

$$\frac{(A_2 + A_3) - (B_2 + B_3)}{(\rho c)_2 + (\rho c)_3} = \frac{A_4}{(\rho c)_4}$$

(4.9)

Force Balance

$$S_2(A_2 + A_3 + B_2 + B_3) = S_4 A_4$$

(4.10)

Figure 4.7: Mathematical description for the force and velocity within Transmission bar-Specimen interface.

From the four expressions given in Figures 4.6 and 4.7 above, eight stress variables exist, A_1, A_2, A_3, A_4, B_1, B_2, B_3 and B_4.

To solve explicitly any of these variables requires an additional expression containing the stress variables. Since no such expression exists, it becomes necessary at this point to define a couple of terms that allow the investigator to extract useful information from the equations.

CHAPTER 5

EXPERIMENTAL WORK

5.1 INTRODUCTION

5.2. Tensile behaviour –welded low carbon steel.

The tensile behaviour of welded low-carbon steel has been studied by many researchers who focused on the behaviour of the three zones (Base metal, Heat Affected Zone and the weld). Apart from using a tensile testing machine, Lee, E. et al (1999) used the acoustic emission (AE) technique to analyze the tensile properties for the welded joint. It was identified that failure occurred at the weld due to excess stress resulting from the presence of residual stress. The level of residual stress reduces from the centre of the weld to the base metal through the Heat Affected Zone.

5.2.1 Objective of the experiment

The objective of the quasi-static test was to determine the maximum strain at which welded specimens (heat-treated and un-heat-treated) fail and hence maximum stress to be used at the range of strains when performing the compression high strain rate experiment with the SHPB. The main purpose of heat treating (annealing) the specimen was to eliminate residual stress induced on the welded part so that the effect of grain sizes on the tensile behaviour of the welded specimen could be determined.

5.2.2 Preparation of Specimens

The tensile strength of the welded low carbon steel was obtained using a standard tensile testing machine. The specimens were prepared in accordance to ASTM standards. Two 20mm diameter by 50mm length steel rods were MIG welded together. Figure 5.1 shows a typical specimen from manufacture to final testing stages.

32
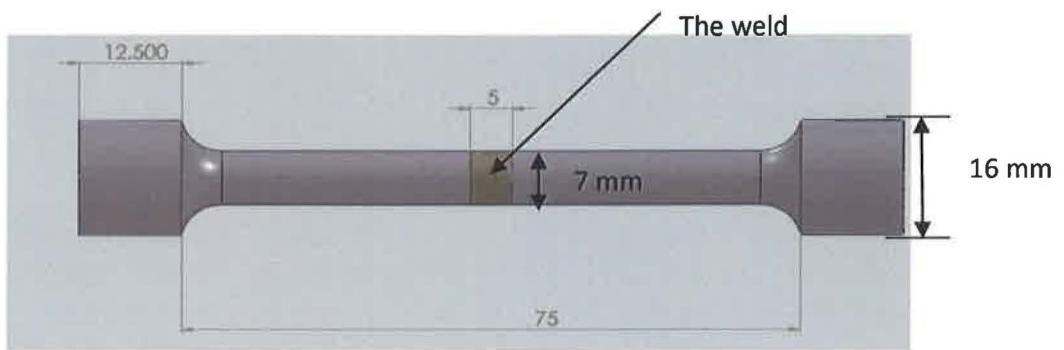
Figure 5.1: Photographs and the sketch of the preparation of the welded specimen for the tensile tests.

Table 5.1 specifications of the weld used.

	Material type	Sizes [mm]	Amount [V and A]	Amount [m/min]	Iron (WT%)	Manganese (WT%)	carbon (WT%)
Welding wire	Low carbon steel (ER705-6)	0.2			>96	1.4	0.15
Voltage			17.4 V				
Feed speed				2.8			
Welding current			200A				
Gas mixture	Argon shielding gas						

After the completion of the welding process, the required standard sizes for the tensile test specimens were fabricated out of the welded bars. The size of specimen used for this test was 7 mm for its throat diameter and 100 mm for its overall length including 65 mm gauge length.

In order to hold a specimen firmly on the tensile machine, a specimen holder was fabricated as shown in figure 5.2. Below is a layout of the specimen holder.
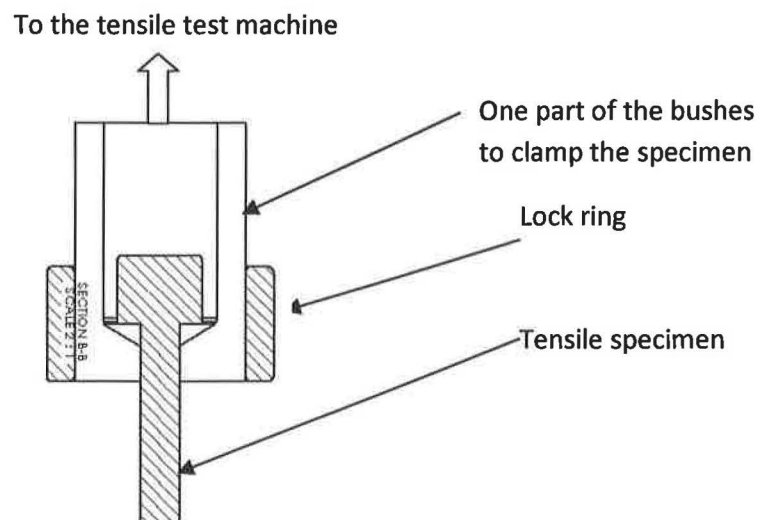
A specimen mounted on the holder

Knuckle joint to the machine's cross head

Lock ring

Bushes to hold the specimen

A screw to hold the two bushes together

Figure 5.2: A specimen holder

5.3   The behaviour of welded low carbon steel under quasi static load.

Quasi-static (tensile test) experiments were conducted for both the heat treated and un-heat-treated welded low carbon steels.   Results were recorded for force versus percentage elongation ($\%\Delta l$) and Nominal Stress (σ) versus nominal strain (ε).

5.3.1   The tensile test Procedure.

A tensile testing machine with a load cell range of 50kN was used for the experiment. Both types of specimens (heat-treated and un-heat treated) were tested using this machine. The fabricated specimens were assembled together with the specially manufactured holder on both ends. The unit was attached on the tensile testing machine. (Initial force was set at 10kN). Force versus percentage elongation results were initially setup from the tensile tester and later converted to Stress versus strain results. The experiment aimed at applying a pulling force until failure occurred. As indicated previously the specimens were welded in the middle (throat area). Practically, both specimens were fractured at the welded points. These points proved to be the weaker points. Figure 5.3 and 5.4 show the fracture zone for the un-heat treated specimen and heat treated specimen respectively.

Welded area fracture point for un- heat treated specimen

Figure 5.3: Photograph of the fractured un-heat-treated welded specimen
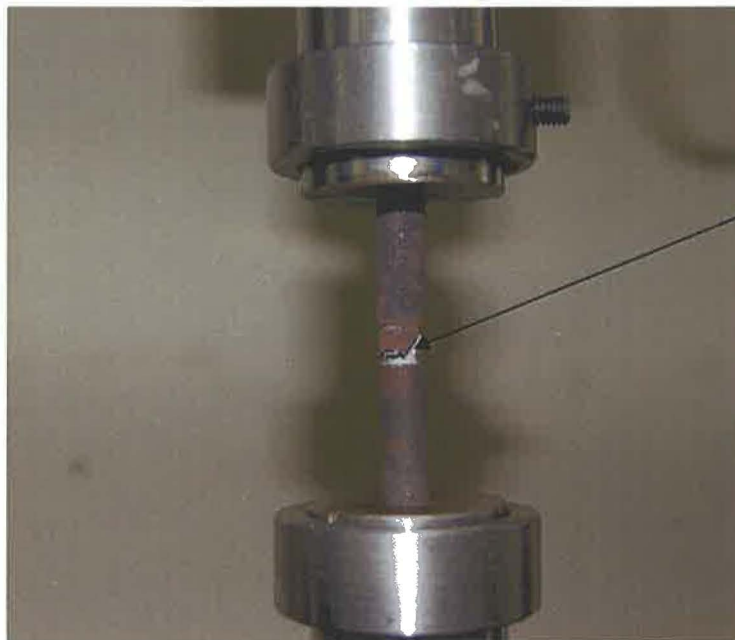
Welded area fracture point for the heat treated specimen

Figure 5.4: Photograph of the fractured heat-treated welded specimen

5.4 Results of the tensile tests on the welded specimen.

5.4.1 Un-heat treated welded specimen

It is seen in Fig 5.5 that the maximum force at UTS was 17.7kN at an elongation of 6.7%. The raw data were converted to stress and strain, Yield and Ultimate strength are shown in figure 5.7.
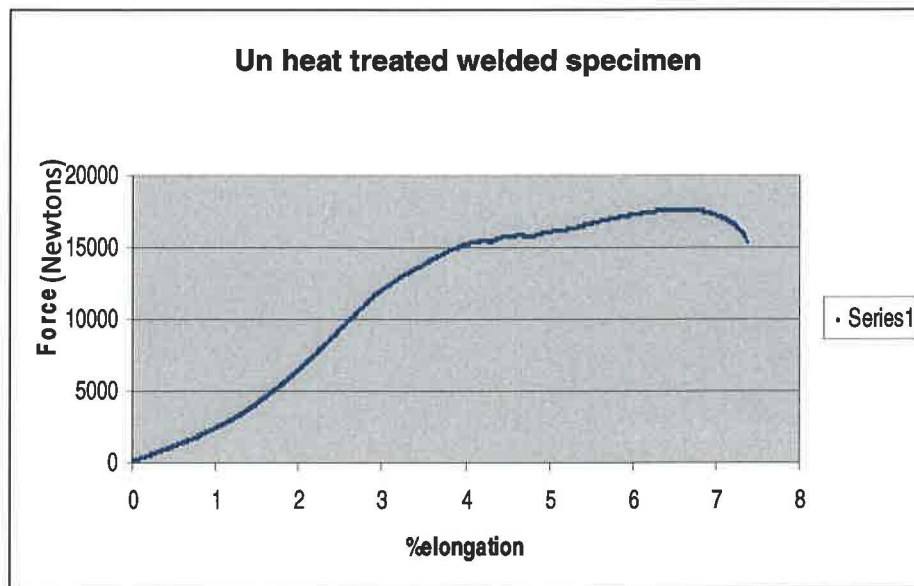

Figure 5.5: Tensile behaviour for the un-heat treated welded mild steel specimen

5.4.2 Heat treated welded specimen

The heat treated welded specimen Yielded at a load of 12.6 kN (Fig 5.6) which is lower than the yield load for the un-heat treated welded specimen (see figure 5.5), however it failed at a higher load (19.2 kN).

The data were converted into Yield and UT stresses and are presented in figure 5.7 and table 5.2 together with the results from the un-heat treated welded specimen for comparison purposes.

The salient feature in comparing the specimens' behaviour is that the annealed (heat treated welded specimen) exhibited lower yield point but higher Ultimate stress than the un-heat treated specimen. This may be explained as follows: Annealing made the specimen more malleable thus yielding at a lower load, however the specimen elongated about twice the amount of the un-heat treated one and due to work hardening while elongating it withstood a higher force before necking and final fracture.
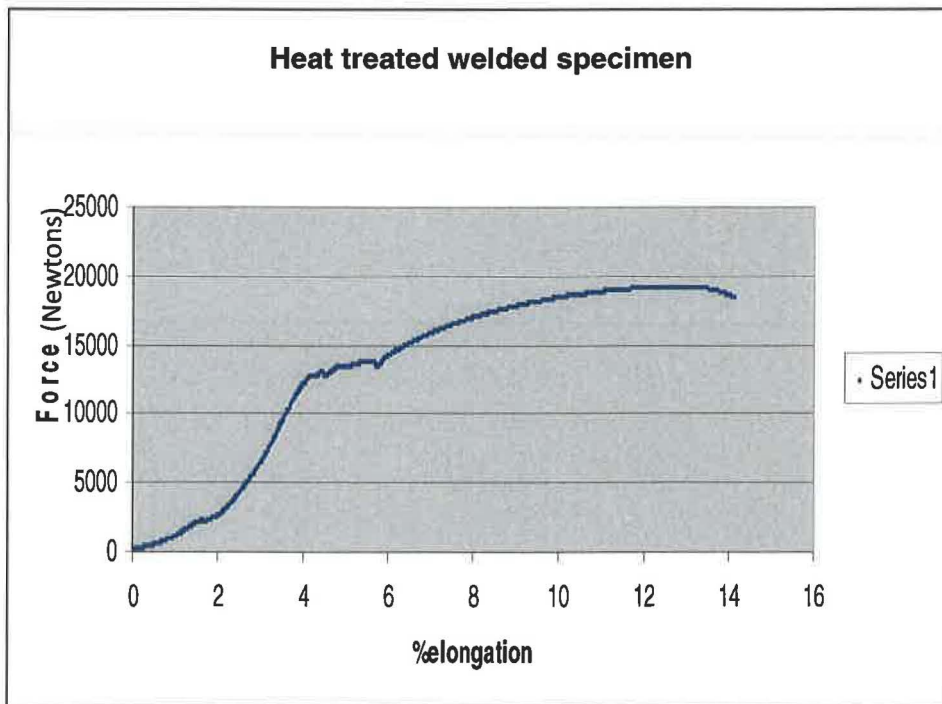
Figure 5.6: Tensile behaviour for the Heat treated welded specimen.

Figure 5.7 shows that the strain for un-heat treated welded specimen at UTS was 0.12 and the UTS was 4.0×10^8 Pa.
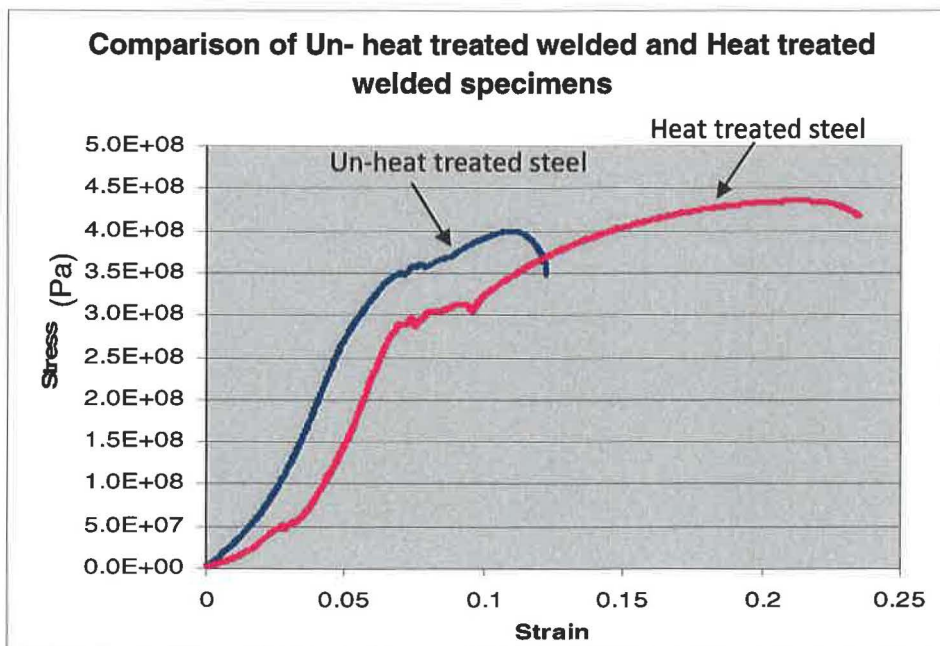

Figure 5.7: Tensile behaviour for both welded specimens.

http://digitalknowledge.cput.ac.za/xmlui/admin/item?administrative-continue=26797318256d703c3c1441213d44042c6042444a&submit_bitstreams